



HAL
open science

A wave of bipotent T/ILC-restricted progenitors shapes the embryonic thymus microenvironment in a time-dependent manner

Ramy Elsaid, Sylvain Meunier, Odile Burlen-Defranoux, Francisca Soares-Da-Silva, Thibaut Perchet, Lorea Iturri, Laina Freyer, Paulo Vieira, Pablo Pereira, Rachel Golub, et al.

► To cite this version:

Ramy Elsaid, Sylvain Meunier, Odile Burlen-Defranoux, Francisca Soares-Da-Silva, Thibaut Perchet, et al.. A wave of bipotent T/ILC-restricted progenitors shapes the embryonic thymus microenvironment in a time-dependent manner. *Blood*, 2020, 10.1182/blood.2020006779 . pasteur-03064548

HAL Id: pasteur-03064548

<https://pasteur.hal.science/pasteur-03064548>

Submitted on 14 Dec 2020

HAL is a multi-disciplinary open access archive for the deposit and dissemination of scientific research documents, whether they are published or not. The documents may come from teaching and research institutions in France or abroad, or from public or private research centers.

L'archive ouverte pluridisciplinaire **HAL**, est destinée au dépôt et à la diffusion de documents scientifiques de niveau recherche, publiés ou non, émanant des établissements d'enseignement et de recherche français ou étrangers, des laboratoires publics ou privés.



American Society of Hematology
2021 L Street NW, Suite 900,
Washington, DC 20036
Phone: 202-776-0544 | Fax 202-776-0545
editorial@hematology.org

A wave of bipotent T/IILC-restricted progenitors shapes the embryonic thymus microenvironment in a time-dependent manner

Tracking no: BLD-2020-006779R2

Ramy Elsaid (Institut Pasteur, France) Sylvain Meunier (Institut Pasteur, France) Odile Burlen-Defranoux (Institut Pasteur, France) Francisca Soares-da-Silva (i3S, Portugal) Thibaut Perchet (Institut Pasteur, France) Lorea Iturri (Paris University, France) Laina Freyer (Institut Pasteur, France) Paulo Vieira (Institut Pasteur, France) Pablo Pereira (Institut Pasteur, France) Rachel GOLUB (Institut Pasteur, France) Antonio Bandeira (Institut Pasteur, France) Elisa Gomez Perdiguero (Institut Pasteur, France) Ana Cumano (Institut Pasteur, France)

Abstract:

During embryonic development, multiple waves of hematopoietic progenitors with distinct lineage potential are differentially regulated in time and space. Two different waves of thymic progenitors colonize the fetal thymus where they contribute to thymic organogenesis and homeostasis. The origin, the lineage differentiation potential of the first wave and their relative contribution in shaping the thymus architecture, remained, however, unclear.

Here we show that the first wave of thymic progenitors comprises a unique population of bipotent cells generating lymphoid tissue inducer, in addition to invariant Vg5⁺ T cells. Transcriptional analysis revealed that innate lymphoid gene signatures and more precisely the lymphoid tissue inducer associated transcripts were expressed in the first but not in the second wave of thymic progenitors. Depletion of early thymic progenitors in a temporally-controlled manner showed that the progeny of the first wave is indispensable for the differentiation of autoimmune regulator expressing medullary thymic epithelial cells. We further show that these progenitors are of strict hematopoietic stem cell origin, despite the overlap between lymphopoiesis initiation and the transient expression of lymphoid associated transcripts in yolk sac erythro-myeloid restricted precursors. Our work highlights the relevance of the developmental timing on the emergence of different lymphoid subsets, required for the establishment of a functionally diverse immune system.

Conflict of interest: No COI declared

COI notes:

Preprint server: Yes; BioRxiv <https://doi.org/10.1101/791103>

Author contributions and disclosures: R.E. designed and performed most experiments, analyzed data and wrote the manuscript; S.M. analyzed chimeric mice and contributed to discussions. F.S.S. and T.P. performed Biomark analysis. O.B.-D performed neonatal thymectomy. E.G.P., L.F. and L.I. performed fate-mapping experiments. A.B. performed adoptive transfer in neonatal mice. R.G., P.V., A.B. and P.P. contributed to the discussions. A.C. directed the research, designed experiments, analyzed data and wrote the manuscript. All authors contributed to the manuscript.

Non-author contributions and disclosures: No;

Agreement to Share Publication-Related Data and Data Sharing Statement: N/A

Clinical trial registration information (if any):

A wave of bipotent T/ILC-restricted progenitors shapes the embryonic thymus microenvironment in a time-dependent manner.

Ramy ELSAID¹⁻³, Sylvain Meunier¹⁻³, Odile Burlen-Defranoux¹⁻³, Francisca Soares-da-Silva^{1,2,6}, Thibaut Perchet¹⁻³, Lorea Iturri^{4,5}, Laina Freyer⁴, Paulo Vieira¹⁻³, Pablo Pereira¹⁻³, Rachel Golub¹⁻³, Antonio Bandeira¹⁻³, Elisa Gomez Perdiguero⁴ & Ana Cumano¹⁻³

¹Unit of Lymphopoiesis, Immunology Department, Institut Pasteur, Paris, France. ²INSERM U1223, Paris, France. ³Université Paris Diderot, Sorbonne Paris Cité, Paris, France.

⁴Macrophages and Endothelial cells group, Development and Stem Cell Biology Department, Institut Pasteur, Paris, France. ⁵Cellule Pasteur UPMC, University Pierre et Marie Curie.

⁶IS – Instituto de Investigação e Inovação em Saúde & INEB – Instituto Nacional de Engenharia Biomédica, Universidade do Porto, 4200-135, Porto, Portugal.

Correspondence should be addressed to A.C. (ana.cumano@pasteur.fr).

Key Points

- Embryonic restricted bipotent T/ILC progenitors shape the thymic architecture by controlling the maturation of mTEC.
- These cells do not originate from yolk sac but rather from intraembryonic derived progenitors.

Abstract

During embryonic development, multiple waves of hematopoietic progenitors with distinct lineage potential are differentially regulated in time and space. Two different waves of thymic progenitors colonize the fetal thymus where they contribute to thymic organogenesis and homeostasis. The origin, the lineage differentiation potential of the first wave and their relative contribution in shaping the thymus architecture, remained, however, unclear.

Here we show that the first wave of thymic progenitors comprises a unique population of bipotent cells generating lymphoid tissue inducer, in addition to invariant $V\gamma 5^+$ T cells. Transcriptional analysis revealed that innate lymphoid gene signatures and more precisely the lymphoid tissue inducer associated transcripts were expressed in the first but not in the second wave of thymic progenitors. Depletion of early thymic progenitors in a temporally-controlled manner showed that the progeny of the first wave is indispensable for the differentiation of autoimmune regulator expressing medullary thymic epithelial cells. We further show that these progenitors are of strict hematopoietic stem cell origin, despite the overlap between lymphopoiesis initiation and the transient expression of lymphoid associated transcripts in yolk sac erythro-myeloid restricted precursors. Our work highlights the relevance of the developmental timing on the emergence of different lymphoid subsets, required for the establishment of a functionally diverse immune system.

Introduction

The embryonic thymus is colonized by two waves of distinct hematopoietic progenitors, named early thymic progenitors (ETP)¹. The first wave of ETP follows a unique developmental program as they share phenotype, transcriptional signature and restricted T cell differentiation potential with HSA^{lo} $\alpha 4\beta 7^-$ fetal liver (FL) common lymphoid progenitors (CLP)^{2,3}. After E15.5, the thymus is colonized by a second wave of ETP that share phenotype, transcriptional signature and differentiation potential with lympho-myeloid primed progenitors (LMPP)²⁻⁵.

Three lymphoid subsets are exclusively developed during embryonic life, the skin resident $V\gamma 5^+$ T cells, the lungs and the genital urinary tract resident $V\gamma 6^+$ and a subset of group 3 innate lymphoid cells (ILC3) known as tissue inducers (LTi)¹. Both $V\gamma 5^+$ T cells and LTi are required for *Aire*⁺ medullary thymic epithelial cells (mTECs) development before birth⁶⁻⁹. *Aire* expression is concomitant with that of CD80, a marker of mTEC maturation, and neonatal *Aire* expression is necessary for inducing life-long T cell tolerance throughout life^{8,10,11}. LTi are also required for secondary lymphoid tissue organization^{12,13} whereas $V\gamma 6$ T cells contribute to tissue remodeling¹⁴.

The majority of embryonic thymic ILCs are LTi, gradually lost after birth and only a small population of ILC2 is maintained throughout life¹⁵. The first ETP generate $V\gamma 5^+$ T cells^{3,16}, however, it is important to determine their origin, whether they generate other embryonic lymphoid cells such as thymic LTi and what is their contribution to shape the thymic architecture in a time-dependent manner⁸.

Most hematopoietic cells are constantly differentiating from hematopoietic stem cells (HSC) although few lineages are HSC independent and exclusively produced during embryonic development^{1,17}. For example, yolk sac (YS) erythro-myeloid progenitors (EMPs) contribute to tissue resident macrophages that persist throughout life¹⁸. This layered organization of the hematopoietic system raises the possibility that, similar to tissue macrophages, the first innate lymphocytes could also be YS derived. Accordingly, cells identified as lympho-myeloid restricted progenitors (LMP) were identified in E9.5 YS before HSC activity is detected¹⁸. They were shown to express lymphoid associated genes (*Il7r*, *Rag2*, *Rag1*) and were proposed as the origin of the first wave of ETP¹⁹. Independent reports have also converged to support the notion that $V\gamma 5^+$ and the $V\gamma 6^+$ T cells, might originate from YS progenitors, independent of HSC^{20,21}. In contrast, $V\gamma 5^+$ and B1a B cells were shown to be preferentially

derived from a particular FL transient HSC-like subset marked by a history of *Flk2* expression²².

In this report, we studied the developmental origin, differentiation potential and the temporal requirement of the first ETP for shaping the thymus microenvironment. We showed, in single cell differentiation assays, that the first ETP comprises bipotent T/LTi progenitors that generate the thymic LTi. Colonization of *Rag2*^{-/-}*γc*^{-/-} thymic lobes with the first, but not the second wave ETP, reconstituted the LTi compartment. Depletion of first wave of lymphoid progenitors resulted in lower numbers of *Vγ5*⁺ T cells, LTi and severely reduced numbers of *CD80*⁺ mTEC, after birth. Therefore, the major role of the first ETP appears to be providing cells that drive thymic organogenesis and tissue homeostasis^{1,10,23}.

We further demonstrated, using an inducible lineage tracer model, that the first ETP originate from HSC. YS-derived progenitors, although showing a history of expression of lymphoid associated genes such as *Il7r*, *Rag2* and *Rag1*, failed to generate a lymphoid progeny in vivo or in vitro. This transient expression, also found in other FL myeloid progenitors, is restricted to embryonic hematopoiesis and uncoupled from differentiation potential. Altogether our data highlight the impact of embryonic developmental timing on lymphocyte production, gene expression, organogenesis and heterogeneity of the immune system.

Methods

(Detailed methods are in the supplemental methods section)

Animals. Mice were bred in house under specific pathogen-free conditions. *Il7r*^{Cre} ²⁴, *Rag2*^{-/-} *γc*^{-/-} *CD45.1* ²⁵, *ROSA26*^{Tomato} ²⁶ and *ROSA26*^{YFP} mice were on C57BL/6 background, *Csf1r*^{MeriCreMer} ²⁷ mice were on FVB background. All animal manipulations were performed according to the French Agriculture ministry and to the European Parliament Directive 2010/63/EU.

Fate-mapping of *Il7r*⁺ hematopoietic progenitors. *Il7r*^{Cre} females were crossed to homozygous *ROSA26*^{YFP}. Indicated embryonic tissues and adult tissues were analyzed by flow cytometry.

Lineage tracing of *Csf1r*⁺ Progenitors. *Csf1r*^{MeriCreMer} were crossed with either *ROSA26*^{YFP} or *ROSA26*^{Tomato} reporter mice. A single dose of 75 μg per g (body weight) of 4-Hydroxytamoxifen (Sigma) (4OHT) injected either at E8.5 or E9.5 induced reporter recombination and was supplemented with 37.5 μg per g (body weight) progesterone (Sigma) (to counteract the mixed estrogen agonist effects of 4OHT)²⁸. To induce recombination at E10.5, females received a single dose of 1.2 mg 4OHT and 0.6 mg progesterone.

In vivo anti-IL7Rα (A7R34) antibody injections. IL-7Rα blockade was performed by three successive intravenously (i.v.) injections of 1 mg anti-IL7Rα antibody (A7R34)²⁹ (a gift from Dr. Shin Nishikawa) in pregnant females at E10.5, E12.5 and E14.5 of gestation.

Results

E13 ETP retain T/LTi lineage potential in vitro and generate LTi cells in a fetal thymic microenvironment

The analysis of the transcriptional profiles of the first (E13) and the second (E18) ETP waves identified the overexpression, in the former, of LTi-associated transcripts (*Rorc*, *Cd4*, *Cxcr5*, *Il1r1* and *Ltb*)^{3,30} (Sup Fig1a). Genes involved in $\gamma\delta$ T cells development (*Bhlhe40*, *Cited4*, *B4galnt2*, *Tgm2* and *Txk*) were also differentially expressed between E13 and E18 ETP (Sup Fig1a). Of note, *Sell* and *Ly6a* were upregulated in E18 ETP, in line with their LMPP affiliation^{2,3}. The E14 DN3 thymocytes were devoid of TdT activity (Sup Fig1b) generating T cells with a restricted T cell repertoire, suggesting that they do not contribute significantly to the adaptive T cell.

We performed a two-step culture^{2,5} (Fig 1a) to detect the potential of single ETP (sorted as in Ramond et al³, $\text{Lin}^- \text{CD117}^+ \text{CD44}^+ \text{CD24}^{\text{low}}$) to generate all major lymphoid lineages (T, B, ILC, NK) and myeloid cells (GM) (Fig 1b). We found that E13 ETP only generated T and ILC whereas E18 ETP retained B and myeloid potential, consistent with our previous observations³. Most ETP gave rise to T and ILCs, although a few (6-15%) only generated T cells and none gave ILCs only. About 59% of the clones derived from E18 ETP generate all subsets of ILC and NK cells in contrast to 24% of E13 ETP (Fig 1b, c), suggesting that E13 ETP have a more restricted differentiation potential.

The striking difference between the two subsets was the high frequency of bipotent T/LTi (22%) precursors only observed in E13 ETP (Fig 1c). Accordingly, a subset of E13-derived ILC3 expressed the LTi marker CCR6 (Fig 1d).

We colonized *Rag2*^{-/-}*γc*^{-/-} non-irradiated fetal thymic organ culture (FTOC) with limited numbers of E13 or E18 ETP and found that only the former could generate thymic LTi (Fig 1d). In addition, only E13 ETP generated $\text{V}\gamma 5^+$ $\gamma\delta$ T cells and both waves generated double positive (DP) thymocytes (Fig 1d), in line with previous report from our laboratory³. To ensure E13 ETP bi-potency in a thymic environment, we repeated the experiment in Figure 1a, and used the expanded progeny of single E13 ETP in *Rag2*^{-/-}*γc*^{-/-} FTOC. Results indicate that 50% of ETP generated $\text{V}\gamma 5$ expressing $\gamma\delta$ T cells and LTi in fetal thymic (Figure 1 e).

Altogether, E12.5-15.5 ETP comprise unique bipotent progenitors, LTi biased, that generate thymic LTi and $V\gamma 5^+ \gamma\delta$ T cells³ within a thymic microenvironment.

First wave ETPs have a LTi primed transcriptional profile

To understand the molecular basis of the E13 ETP LTi lineage potential, we performed single-cell transcriptional analysis by multiplex qRT-PCR for the expression of 41 lymphoid-associated genes. Unsupervised hierarchical clustering identified 4 distinct clusters (Fig 2a). Cluster I, comprising a majority (76%) of E18 ETP, showed no ILC transcript expression indicating that they are not primed toward a specific ILC lineage, consistent with their multipotent ILC differentiation capacity. E13 ETP, found in Clusters II and IV, expressed the ILC associated transcripts *Tox*, *Tcf7* and *Gata3*. Expression of LTi transcripts *Cxcr6*, *Cd4*, *Rorc*, *Cxcr5*, *Il1r1* and *Ltb* was found in cells within Cluster IV, consistent with a LTi differentiation potential.

Cells in Cluster II expressed *Zbtb16*, *Gzmb*, *Nfil3*, *Itga2b* and *Gzma* associated with innate-like T cells³¹. Cluster III comprised two thirds of E13 and one third of E18 ETP and was characterized by the of lower expression of *Tox*, *Gata3*, *Tcf7*, *Sox4*, *Runx1* and *Runx3* indicative of common ILC priming and consistent with a broad ILC differentiation potential (Fig 2a). Altogether, these results indicated that the first ETP are unique in expressing LTi and invariant T cells transcripts, indicative of transcriptional priming.

First wave ETPs contribute to the maturation of the thymic mTEC

To assess the role of the first ETP and their progeny in mTEC maturation, we used in vivo injection of A7R34 anti-IL7R α ³²⁻³⁴ antibody in pregnant females. We injected A7R34 antibody at E10.5, E12.5 and E14.5, and analyzed the embryos at E16.6 and P2 newborn mice. At E16.5 we observed severely reduced numbers of $V\gamma 5^+$ T and LTi cells in the thymus although the second wave ETP³ were not altered (Fig 2b).

At P2 treated mice had normal numbers of DN thymocytes consistent with an unaffected second wave of thymic colonization. P2 had significantly lower numbers of $V\gamma 5^+$ T, and drastically lower numbers of LTi, compared to controls, indicating efficient depletion of the first ETP and their progeny (Fig 2b). Interestingly, CD80⁺ mTEC (mature *Aire* expressing cells)⁸ were reduced of around 3-fold indicating that the first ETP are required for mTEC maturation, around birth. CD4⁺CD8⁺ double positive (DP) cells were also reduced by less than three-fold. Our results indicate that the progeny of the first wave ETP contribute to mTEC maturation, required for conventional T cell negative selection.

Neonatal thymectomy does not impact numbers of tissue resident $V\gamma 5^+$ and $V\gamma 6^+$ $\gamma\delta$ T cells

$V\gamma 5^+$ and $V\gamma 6^+$ $\gamma\delta$ T cells in the skin and in the lymph nodes (LN), respectively, are of embryonic origin^{16,35}, although they develop asynchronously. To assess the dependency of these $\gamma\delta$ subsets on thymic output, indicating their origin in the first or second wave of ETP, we performed neonatal thymectomy. Six weeks after neonatal thymectomy or sham-operation as control (Fig 3a), complete thymectomy was ascertained by the absence of double positive CD4/CD8 cells in the tissue around the thymus location (Fig 3b). Thymectomized mice (n=6) were severely lymphopenic as shown by the numbers of CD4 and CD8 $\alpha\beta$ T cells in the inguinal (i) lymph node (LN) (Fig 3d) and in the spleen. Splenic CD44⁻ $\alpha\beta$ T cells were severely reduced (Fig 3e), a sign of activation of the T cell compartment consequent to the lymphopenia and consistent with the absence of a functional thymus in these mice. The numbers of $V\gamma 5^+$ $\gamma\delta$ T cells in the skin and of iLN $V\gamma 4^-$ IL17 producing $\gamma\delta$ T cells (considered as $V\gamma 6^+$) were similar in sham and in thymectomized animals (Fig 3c, d). By contrast, iLN $V\gamma 4^+$ IL-17 producing $\gamma\delta$ T cells were severely reduced (Fig 3d). These experiments suggest that these two embryonic $\gamma\delta$ T cell subsets are likely derived from the first wave ETPs. All other $\alpha\beta$ or $\gamma\delta$ T depend on post-natal thymic output and thus are issued from the second wave of ETP.

Embryonic ETP have multi-ILC lineage potential *in vivo*

To assess E13 and E18 ETP ILC lineage potential *in vivo*, CD45.2⁺ E13 or E18 ETP were intravenously transferred into 1-day old CD45.1⁺ Rag2^{-/-} $\gamma c^{-/-}$ mice and E13 fetal liver HSCs (Lin⁻ CD117⁺ Sca-1⁺ CD150⁺ CD48⁻) were used as a positive control (Sup Fig 2a). Five weeks after transfer³⁶, mice engrafted with HSCs and E18 ETP developed B cells, ILC and myeloid cells (Sup Fig 2c and data not shown). By contrast, mice engrafted with E13 ETP generated only ILC (Sup Fig 2b), consistent with the E13 ETP restricted lymphoid potential. Analysis of PB 3 and 6 weeks or splenic cells 5 weeks, after transplantation show a total absence of B and myeloid progeny from E13 ETP (Sup Fig 2b, e). Few T cells were generated in these chimeras because Rag2^{-/-} $\gamma c^{-/-}$ mice have an atrophic thymus and ETP down-regulate

CCR7 and CCR9 once in the thymus, consequently losing their ability to home back to the thymus³⁷.

Analysis of intestinal lamina propria, where all ILC lineages coexist, showed that both waves ETP generated NK cells (EOMES⁺), ILC1 (EOMES⁻), ILC3 (RORγt⁺) and ILC2 (GATA3⁺). In the lung we found ILC2, in the spleen NK cells and in the liver NK cells and ILC1 (Sup Fig 2c, d). These results indicated that E13 and E18 ETP have the capacity to generate all ILC subsets *in vivo* recapitulating the expected tissue distribution.

Emergence of *Il7r* expressing YS-progenitors in E9.5 embryos

We used a lineage tracer mouse line, *Il7ra*^{Cre}Rosa26^{YFP38} to identify the origin of the first *Il7r*⁺ ETPs. YFP expressing cells were undetectable in E8.5 embryos, in YS and embryo proper, in either the Kit⁺ or Kit⁻ fraction (data not shown). Consistent with previous studies, YFP⁺ progenitors were first detected in Lin⁻Kit⁺CD41⁺ E9.5 YS (Fig 4a, b, c) and undetected in the AGM or in the placenta (Fig 4d). 5-8 % of the c-kit⁺ YS cells were YFP⁺ (Fig 4b, c) expressed CD31, CD16/32 and lacked surface expression of CD115, CD127, CD135, the phenotype of YS EMPs (Lin⁻Kit⁺CD41⁺YFP⁻)(Fig 4e)^{39,40}.

To investigate the lineage potential of YS YFP⁺ cells, single cells were cultured into monolayers of OP9-DL4 (T/GM) or OP9 (B/GM) stroma (Fig 4f). While YFP⁺ YS cells showed myeloid potential, they lacked detectable T or B cell potential (Fig 4g, h). Liquid-culture colony assays showed that both YFP⁺ and YFP⁻ Lin⁻Kit⁺ YS cells exhibited comparable GM and MkE potential (Fig 4i). These results indicated that YFP expression in the E9.5 YS embryos does not equate with lymphoid potential, and both YFP⁺ and YFP⁻ E9.5 YS Kit⁺ cells showed a lineage potential similar to EMP^{28,39,40}.

E9.5 YS-derived cells did not generate Vγ5⁺ T cells or initiate thymopoiesis, whereas E10.5 YS-Kit⁺ progenitors and E12 FL LSK readily generated T cells including Vγ5⁺ T cells in fetal thymic organ cultures (FTOCs) of thymic lobes (Fig 4j). E10.5 YS-Kit⁺ progenitor derived T cells originate from AGM pre-HSC, known to enter circulation between E9.5 and E11.5^{41,42} and were used to probe the sensitivity of the T cell assay.

These experiments showed that E9.5 YS progenitors are devoid of lymphoid potential under culture conditions sufficiently sensitive to detect few circulating T cell progenitors.

Expression of lymphoid associated transcripts in YS progenitors is transient.

To further characterize YFP⁺ YS progenitors, we analyzed the expression of transcripts associated with multiple hematopoietic lineages in single E9.5 YS YFP⁺ and YFP⁻ Lin⁻

CD117⁺CD41⁺ cells. Unsupervised hierarchical clustering did not segregate YFP⁺ and YFP⁻ cells indicating that they do not differ significantly in the expression of the analyzed transcripts (Fig 5a). Cluster I associated *Pu-1*, *Irf8* and *Csf1r* expressions with low or no *Kdr*, *Tek*, *Runx1*, *Mp*, *Foxo1*, *IL7ra* and *Flk2* expressing cells, a pattern of expression corresponding to EMPs⁴³ (Fig 5a). Cluster II singled out EMP expressing *Pu-1*, *Irf8* and *Csf1r* but also *Kdr*, *Tek*, *Runx1*, *Mpl* and *Foxo1*, suggesting recent specification from hemogenic endothelium⁴³⁻⁴⁵. These cells also exhibited *Il7ra* and *Flk2*. Clusters III and IV comprised YFP⁺ and YFP⁻ cells with high levels of *Gata1* indicating their erythroid lineage engagement. Cells in cluster IV also expressed *Klf1* indicating that they are more advanced into the erythroid lineage differentiation. As expected, no lymphoid associated transcripts were detected in cells from cluster III and IV. *Ebf1*, *Pax5* or *Rag1* were not detected in any of the analyzed YS cells. Within the 47 YFP⁺ cells analyzed only 6 co-expressed *Il7ra* transcripts reinforcing the notion that *Il7ra* expression is transient in E9.5 YS progenitors (Fig 5b). Interestingly, analyzed at the population level, YFP⁺ cells expressed significantly higher levels of *Rag1*, *Rag2* and *Il7r* than YFP⁻ cells albeit 10-fold lower than CLP (Sup Fig 3). These experiments indicated that expression of lymphoid associated genes in emerging YS-derived EMP is transient and dissociated from differentiation potential.

Multiple FL hematopoietic progenitors express lymphoid associated genes.

We further assessed whether YFP expression also occurs in other embryonic hematopoietic cells. We found that unlike in adult bone marrow (BM)³⁸, YFP expression in the FL was found in multipotent and myeloid progenitors (Sup Fig 4a, b). FL and fetal blood (FB), short-term HSC (ST-HSCs), multipotent progenitors (MPP), granulocyte-monocyte progenitors (GMP), common myeloid progenitors (CMP) and megakaryocytes-erythroid progenitors (MEP) were labeled at frequencies ranging from 10%-40% (Sup Fig 4a, b; Sup Figure 5 for gating strategy). The frequency of YFP⁺ ST-HSC and myeloid progenitors progressively decreased after birth and was undetectable in adult mice³⁸ (Sup Fig 4b). FL YFP⁺ GMP and CMP also lacked any detectable B cell potential *in vitro* (Sup Fig 4c).

We found that 40% of E18 brain microglia, the FL Kupffer cells and the skin mast and Langerhans cells also expressed YFP, in line with a recent report⁴⁶ (Sup Fig 6a, b). These observations indicated that this model does not faithfully trace the origin of embryonic lymphoid cells.

Thymopoiesis-initiating cells develop exclusively from HSC-derived progenitors

To define the origin of the first ETP, we used a fate mapping mouse model expressing the tamoxifen inducible Cre (*MerCreMer*) under the control of the *Csf1r* promoter²⁷ (Fig 6a). Injection of hydroxy-tamoxifen (4-OH-TAM) in either *Csf1r*^{MerCreMer}*Rosa26*^{YFP} or *Rosa26*^{Tomato} (depending on the availability of fluorochrome-labelled antibodies for the analysis) induced recombination and permanently labelled *Csf1r* expressing cells and their progeny. *Csf1r* is first expressed in E8.5 YS progenitors²⁸, later it is expressed in E9.5 YS *Il7ra*^{Cre}*Rosa26*^{YFP} (Fig 5a, Sup Fig 3)¹⁸ and at E10.5 *Csf1r* is also expressed in pre-HSC⁴⁴ (Sup Fig 7d).

In embryos pulsed at E8.5, YFP⁺ cells were detected in the E9.5 YS, expressed *Csf1r*, *Il7r* and were devoid of lymphoid potential (Sup Fig 7a, b, c). In embryos pulsed at either E8.5 or E9.5 and analyzed at E12.5, YFP⁺ HSC, HSC-derived lymphoid progenitors and ETP were either not detectable or represented less than 1% in FL and thymus, respectively (Fig 6b, c). In contrast, 30-50% of microglia cells were labeled, indicating the labeling efficiency. Embryos pulsed at E10.5 and analyzed at E12.5 showed significant labeling in populations of FL HSC, multipotent, lymphoid and myeloid progenitors (Fig 6c). Interestingly, the frequency of Tomato⁺ cells in E12.5 ETP (25%) and in FL LTi (22%) (Sup Fig 7e for gating strategy) paralleled that of HSC (31%).

These fate-mapping experiments demonstrated that under physiological conditions no detectable ETP or lymphoid progenitor originate from YS cells, rather their origin is coincident in time with that of pre-HSC.

Innate-like V γ 5⁺ T cells or B1-a cells that differentiate during a limited time window of embryonic development have been proposed to derive from HSC-independent precursors.

Adult *Csf1r*^{MerCreMer} *Rosa26*^{YFP} or *Csf1r*^{MerCreMer} *Rosa26*^{Tomato} mice pulsed at E8.5 showed no YFP labelled lymphocytes and those pulsed at E9.5 showed less than 1% of V γ 5⁺ T or B-1a labelled cells. In both cases, 30-40% of microglia cells were YFP labelled (Fig 6c). Embryos pulsed at E10.5 showed a frequency of V γ 5⁺ T or B-1a labelled cells similar to that found in HSC (Fig 6c) (Sup Fig 7f for gating strategy). These results are consistent with a strict HSC origin of all lymphoid cells including the first wave of ETP and innate-like lymphocytes of embryonic origin.

Discussion

Here we show that the first ETP comprise a unique and novel population of bipotent cells that generate the invariant T and LTi lineages, and together induce the maturation of medullary thymic epithelial cells^{8,9}. This observation was further supported by a transcriptional analysis showing a cluster of E13.5 ETP that are primed towards the LTi lineage with high expression of *Rorc*, *Cd4*, *Cxcr5*, *Il1r1* and *Ltb*³⁰. The first ETP were devoid of TdT activity giving rise to T cells without N sequences and thus with a restricted T cell repertoire. Low TdT expression together with the poor proliferative capacity³, suggested that the contribution of the first ETP to the conventional T cell compartment is limited¹. Together these observations indicate that the first wave of ETP is dedicated to induce early maturation of the thymic epithelia and to generate invariant T cells that ensure tissue homeostasis. Neonatal *Aire* expression is necessary for inducing life-long T cell tolerance¹¹ and it was shown that both $V\gamma 5^+ \gamma\delta$ cells and LTi play an important role in the maturation of $CD80^+mTEC$ ⁸. Our results highlight the necessity of a normal development of the first ETP and their progeny to ensure *Aire* expression at birth and therefore induction of neonatal thymic tolerance and avoiding autoimmunity. A recent report analyzing human embryonic thymopoiesis suggests that similar sequence of events might be shared between mouse and human⁴⁷.

Using *Rag1*-GFP mice, it was argued that E11.5 ETPs retained myeloid potential and resembled PIRA/B⁺ LMPPs in phenotype, lineage potential and molecular signature¹⁹. Our data show that the first ETP, isolated using generally accepted surface markers^{3,48} and not based on reporter mouse models, are T/ILC restricted with poor B and myeloid potential.

The analysis of YFP⁺ cells under the control of the *Il7r* regulatory sequences throughout embryonic life indicated that, unlike adult hematopoietic progenitors, multipotent and myeloid restricted progenitors express lymphoid associated genes, albeit in a transient manner, without any consequent restriction in their differentiation potential^{46,49,50}. This data argues against the notion that the embryonic thymus is initially seeded at E11.5 by *Rag1*-expressing lympho-myeloid restricted progenitors¹⁹. These observations established that in hematopoiesis, gene expression does not necessarily equate with lineage potential and care

should be taken before extrapolating to embryonic development findings obtained by the analysis of adult hematopoiesis.

By analogy with tissue resident macrophages^{17,51}, it was proposed that also early developing innate-like T cells and therefore the first ETP were HSC independent^{18–21,52–54}. Inducible lineage tracing of *Cdh5* and *Runx1* expressing cells²⁰ suggested that $V\gamma 5^+$ T cells were generated from YS-derived hematopoietic progenitors. *Cdh5*, *Runx1* and *Tie2* are expressed in endothelial cells of both the YS, that produces EMP, and the AGM that is the source of HSC⁵⁵. Therefore, endothelial cells and their hematopoietic progeny will be labeled in both generation sites with different frequencies at different induction time points^{20,51,56–58}. To unambiguously assign the contribution of each anatomical site to blood cell formation, we used *Csf1r*^{MeriCreMer} lineage tracing model that marks the progeny of cells generated in each of these hematopoietic sites in a non-overlapping spatio-temporal manner. Recombination induced at E8.5-E9.5 marks the YS derived progenitors (including lymphoid-associated gene expressing progenitors), in which virtually no $V\gamma 5^+$ T cells or early ETP were labeled. Recombination induced at E10.5 traced both YS-derived *Csf1r*⁺ myeloid cells, HSC and also E12.5 ETP and CLP, and adult $V\gamma 5^+$ $\gamma\delta$ T cells and B1a B cells. These experiments are the first *in vivo* evidence that ETP, innate-like lymphocytes and lymphoid progenitors originate in the embryo from *Csf1r*⁺ HSCs-derived progeny. However compelling, these results are also compatible with a late expression of *Csf1r* in subsets of YS cells. We think that this is unlikely because induction at E9.5 leads to virtually no contribution of *Csf1r*⁺ cells to the lymphoid compartment which would be expected from an ongoing process and because it was previously reported that between E9 and E11 the frequency of *Csf1r*⁺ YS cells continuously decrease⁵⁶. It is however possible that AGM derived multipotent progenitors bypass the HSC stage and directly differentiate and contribute to the first wave ETP, as recently reported in Zebrafish⁵⁹ and in mice⁵². Altogether, these data indicate that lymphopoiesis is a hallmark of HSC and HSC-derived progenitors.

The ability of adult ETP to generate ILCs *in vitro* has been previously documented^{31,60,61}, however the capacity of E13 ETP to generate thymic LTi within a thymic microenvironment is the first evidence that these cells can originate also from hematopoietic progenitors other than the classical ILCP^{62,63}, and in organs other than the FL where hematopoiesis occurs⁶⁴ (Fig 7).

This highly orchestrated sequence of events highlights the requirement of a layered immune cell production whereby the first wave of ETP is essential for thymic organogenesis and T cell tolerance.

References:

1. Cumano A, Berthault C, Ramond C, et al. New Molecular Insights into Immune Cell Development. *Annu. Rev. Immunol.* 2019;37(1):497–519.
2. Berthault C, Ramond C, Burlen-Defranoux O, et al. Asynchronous lineage priming determines commitment to T cell and B cell lineages in fetal liver. *Nat. Immunol.* 2017;18(10):1139–1149.
3. Ramond C, Berthault C, Burlen-Defranoux O, et al. Two waves of distinct hematopoietic progenitor cells colonize the fetal thymus. *Nat. Immunol.* 2013;15(1):27–35.
4. Bhandoola A, von Boehmer H, Petrie HT, Zúñiga-Pflücker JC. Commitment and Developmental Potential of Extrathymic and Intrathymic T Cell Precursors: Plenty to Choose from. *Immunity.* 2007;26(6):678–689.
5. Luc S, Luis TC, Boukarabila H, et al. The earliest thymic T cell progenitors sustain B cell and myeloid lineage potential. *Nat. Immunol.* 2012;13(4):412–419.
6. Alves NL, Takahama Y, Ohigashi I, et al. Serial progression of cortical and medullary thymic epithelial microenvironments. *Eur. J. Immunol.* 2014;44(1):16–22.
7. Boyden LM, Lewis JM, Barbee SD, et al. Skint1, the prototype of a newly identified immunoglobulin superfamily gene cluster, positively selects epidermal gammadelta T cells. *Nat. Genet.* 2008;40(5):656–662.
8. Roberts NA, White AJ, Jenkinson WE, et al. Rank signaling links the development of invariant $\gamma\delta$ T cell progenitors and Aire(+) medullary epithelium. *Immunity.* 2012;36(3):427–437.
9. Rossi SW, Kim M-Y, Leibbrandt A, et al. RANK signals from CD4+3- inducer cells regulate development of Aire-expressing epithelial cells in the thymic medulla. *J. Exp. Med.* 2007;204(6):1267–1272.
10. Abramson J, Anderson G. Thymic Epithelial Cells. *Annu. Rev. Immunol.* 2017;35(1):85–118.
11. Guerau-de-Arellano M, Martinic M, Benoist C, Mathis D. Neonatal tolerance revisited: a perinatal window for Aire control of autoimmunity. *J. Exp. Med.* 2009;206(6):1245–1252.
12. Cupedo T, Mebius RE. Role of chemokines in the development of secondary and tertiary lymphoid tissues. *Semin. Immunol.* 2003;15(5):243–248.
13. Cupedo T, Kraal G, Mebius RE. The role of CD45+CD4+CD3- cells in lymphoid organ development. *Immunol. Rev.* 2002;189:41–50.
14. Papotto PH, Ribot JC, Silva-Santos B. IL-17+ $\gamma\delta$ T cells as kick-starters of

inflammation. *Nat. Immunol.* 2017;18(6):604–611.

15. Jones R, Cosway EJ, Willis C, et al. Dynamic changes in intrathymic ILC populations during murine neonatal development. *Eur. J. Immunol.* 2018;48(9):1481–1491.

16. Ikuta K, Kina T, MacNeil I, et al. A developmental switch in thymic lymphocyte maturation potential occurs at the level of hematopoietic stem cells. *Cell.* 1990;62(5):863–874.

17. Perdiguero EG, Geissmann F. The development and maintenance of resident macrophages. *Nat. Immunol.* 2016;17(1):2–8.

18. Böiers C, Carrelha J, Lutteropp M, et al. Lymphomyeloid Contribution of an Immune-Restricted Progenitor Emerging Prior to Definitive Hematopoietic Stem Cells. *Cell Stem Cell.* 2013;13(5):535–548.

19. Luis TC, Luc S, Mizukami T, et al. Initial seeding of the embryonic thymus by immune-restricted lympho-myeloid progenitors. *Nat. Immunol.* 2016;17(12):1424–1435.

20. Gentek R, Ghigo C, Hoeffel G, et al. Epidermal $\gamma\delta$ T cells originate from yolk sac hematopoiesis and clonally self-renew in the adult. *J. Exp. Med.* 2018;215(12):2994–3005.

21. Spidale NA, Sylvia K, Narayan K, et al. Interleukin-17-Producing $\gamma\delta$ T Cells Originate from SOX13+ Progenitors that Are Independent of $\gamma\delta$ TCR Signaling. *Immunity.* 2018;49(5):857–872.e5.

22. Beaudin AE, Boyer SW, Perez-Cunningham J, et al. A Transient Developmental Hematopoietic Stem Cell Gives Rise to Innate-like B and T Cells. *Cell Stem Cell.* 2016;19(6):768–783.

23. White AJ, Lucas B, Jenkinson WE, Anderson G. Invariant NKT Cells and Control of the Thymus Medulla. *J. Immunol. Baltim. Md 1950.* 2018;200(10):3333–3339.

24. Schlenner SM, Madan V, Busch K, et al. Fate Mapping Reveals Separate Origins of T Cells and Myeloid Lineages in the Thymus. *Immunity.* 2010;32(3):426–436.

25. Colucci F, Soudais C, Rosmaraki E, et al. Dissecting NK cell development using a novel alymphoid mouse model: investigating the role of the c-abl proto-oncogene in murine NK cell differentiation. *J. Immunol. Baltim. Md 1950.* 1999;162(5):2761–2765.

26. Madisen L, Zwingman TA, Sunkin SM, et al. A robust and high-throughput Cre reporting and characterization system for the whole mouse brain. *Nat. Neurosci.* 2010;13(1):133–140.

27. Qian B-Z, Li J, Zhang H, et al. CCL2 recruits inflammatory monocytes to facilitate breast-tumour metastasis. *Nature.* 2011;475(7355):222–225.

28. Gomez Perdiguero E, Klapproth K, Schulz C, et al. Tissue-resident macrophages originate from yolk-sac-derived erythro-myeloid progenitors. *Nature.* 2015;518(7540):547–551.

29. Sudo T, Nishikawa S, Ohno N, et al. Expression and function of the interleukin 7 receptor in murine lymphocytes. *Proc. Natl. Acad. Sci.* 1993;90(19):9125–9129.

30. Ishizuka IE, Chea S, Gudjonson H, et al. Single-cell analysis defines the divergence between the innate lymphoid cell lineage and lymphoid tissue-inducer cell lineage. *Nat. Immunol.* 2016;17(3):269–276.

31. De Obaldia ME, Bhandoola A. Transcriptional Regulation of Innate and Adaptive Lymphocyte Lineages. *Annu. Rev. Immunol.* 2015;33(1):607–642.

32. Yoshida H, Kawamoto H, Santee SM, et al. Expression of alpha(4)beta(7) integrin defines a distinct pathway of lymphoid progenitors committed to T cells, fetal intestinal lymphotoxin producer, NK, and dendritic cells. *J. Immunol. Baltim. Md 1950.* 2001;167(5):2511–2521.

33. Hashizume T, Togawa A, Nochi T, et al. Peyer's Patches Are Required for Intestinal Immunoglobulin A Responses to Salmonella spp. *Infect. Immun.* 2008;76(3):927–934.

34. Schneider C, Lee J, Koga S, et al. Tissue-Resident Group 2 Innate Lymphoid Cells

Differentiate by Layered Ontogeny and In Situ Perinatal Priming. *Immunity*. 2019;50(6):1425-1438.e5.

35. Haas JD, Ravens S, Düber S, et al. Development of Interleukin-17-Producing $\gamma\delta$ T Cells Is Restricted to a Functional Embryonic Wave. *Immunity*. 2012;37(1):48–59.
36. Xu W, Cherrier DE, Chea S, et al. An Id2RFP-Reporter Mouse Redefines Innate Lymphoid Cell Precursor Potentials. *Immunity*. 2019;
37. Zlotoff DA, Sambandam A, Logan TD, et al. CCR7 and CCR9 together recruit hematopoietic progenitors to the adult thymus. *Blood*. 2010;115(10):1897–1905.
38. Schlenner SM, Madan V, Busch K, et al. Fate Mapping Reveals Separate Origins of T Cells and Myeloid Lineages in the Thymus. *Immunity*. 2010;32(3):426–436.
39. Bertrand JY. Three pathways to mature macrophages in the early mouse yolk sac. *Blood*. 2005;106(9):3004–3011.
40. McGrath KE, Frame JM, Fegan KH, et al. Distinct Sources of Hematopoietic Progenitors Emerge before HSCs and Provide Functional Blood Cells in the Mammalian Embryo. *Cell Rep*. 2015;11(12):1892–1904.
41. Delassus S, Cumano A. Circulation of Hematopoietic Progenitors in the Mouse Embryo. *Immunity*. 1996;4(1):97–106.
42. McGrath KE, Koniski AD, Malik J, Palis J. Circulation is established in a stepwise pattern in the mammalian embryo. *Blood*. 2003;101(5):1669–1675.
43. Mass E, Ballesteros I, Farlik M, et al. Specification of tissue-resident macrophages during organogenesis. *Science*. 2016;353(6304):.
44. Baron CS, Kester L, Klaus A, et al. Single-cell transcriptomics reveal the dynamic of haematopoietic stem cell production in the aorta. *Nat. Commun*. 2018;9(1):.
45. Kasaai B, Caolo V, Peacock HM, et al. Erythro-myeloid progenitors can differentiate from endothelial cells and modulate embryonic vascular remodeling. *Sci. Rep*. 2017;7:43817.
46. Leung GA, Cool T, Valencia CH, et al. The lymphoid-associated interleukin 7 receptor (IL7R) regulates tissue-resident macrophage development. *Dev. Camb. Engl*. 2019;146(14):.
47. Tieppo P, Papadopoulou M, Gatti D, et al. The human fetal thymus generates invariant effector $\gamma\delta$ T cells. *J. Exp. Med*. 2020;217(3):.
48. Porritt HE, Rumpf LL, Tabrizifard S, et al. Heterogeneity among DN1 Prothymocytes Reveals Multiple Progenitors with Different Capacities to Generate T Cell and Non-T Cell Lineages. *Immunity*. 2004;20(6):735–745.
49. Gautier EL, Shay T, Miller J, et al. Gene-expression profiles and transcriptional regulatory pathways that underlie the identity and diversity of mouse tissue macrophages. *Nat. Immunol*. 2012;13(11):1118–1128.
50. Heng TSP, Painter MW, Immunological Genome Project Consortium. The Immunological Genome Project: networks of gene expression in immune cells. *Nat. Immunol*. 2008;9(10):1091–1094.
51. Gomez Perdiguero E, Klapproth K, Schulz C, et al. Tissue-resident macrophages originate from yolk-sac-derived erythro-myeloid progenitors. *Nature*. 2015;518(7540):547–551.
52. Kobayashi M, Shelley WC, Seo W, et al. Functional B-1 progenitor cells are present in the hematopoietic stem cell-deficient embryo and depend on Cbf for their development. *Proc. Natl. Acad. Sci*. 2014;111(33):12151–12156.
53. Yoshimoto M, Montecino-Rodriguez E, Ferkowicz MJ, et al. Embryonic day 9 yolk sac and intra-embryonic hemogenic endothelium independently generate a B-1 and marginal zone progenitor lacking B-2 potential. *Proc. Natl. Acad. Sci. U. S. A*. 2011;108(4):1468–1473.
54. Yoshimoto M, Porayette P, Glosso NL, et al. Autonomous murine T-cell progenitor production in the extra-embryonic yolk sac before HSC emergence. *Blood*.

2012;119(24):5706–5714.

55. Elsaid R, Yang J, Cumano A. The influence of space and time on the establishment of B cell identity. *Biomed. J.* 2019;

56. Hoeffel G, Chen J, Lavin Y, et al. C-Myb+ Erythro-Myeloid Progenitor-Derived Fetal Monocytes Give Rise to Adult Tissue-Resident Macrophages. *Immunity.* 2015;42(4):665–678.

57. Gentek R, Ghigo C, Hoeffel G, et al. Hemogenic Endothelial Fate Mapping Reveals Dual Developmental Origin of Mast Cells. *Immunity.* 2018;48(6):1160-1171.e5.

58. Busch K, Klapproth K, Barile M, et al. Fundamental properties of unperturbed haematopoiesis from stem cells in vivo. *Nature.* 2015;518(7540):542–546.

59. Tian Y, Xu J, Feng S, et al. The first wave of T lymphopoiesis in zebrafish arises from aorta endothelium independent of hematopoietic stem cells. *J. Exp. Med.* 2017;jem.20170488.

60. Wong SH, Walker JA, Jolin HE, et al. Transcription factor ROR α is critical for nuocyte development. *Nat. Immunol.* 2012;13(3):229–236.

61. Yang Q, Li F, Harly C, et al. TCF-1 upregulation identifies early innate lymphoid progenitors in the bone marrow. *Nat. Immunol.* 2015;16(10):1044–1050.

62. Diefenbach A, Gnafakis S, Shomrat O. Innate Lymphoid Cell-Epithelial Cell Modules Sustain Intestinal Homeostasis. *Immunity.* 2020;52(3):452–463.

63. Diefenbach A, Colonna M, Koyasu S. Development, Differentiation, and Diversity of Innate Lymphoid Cells. *Immunity.* 2014;41(3):354–365.

64. Cumano A, Godin I. Ontogeny of the Hematopoietic System. *Annu. Rev. Immunol.* 2007;25(1):745–785.

ACKNOWLEDGMENTS

We thank S. Novault, S. Megharba and S. Schmutz from the flow cytometry core facility of the Institut Pasteur for technical support; the staff of the animal facility of the Institut Pasteur for mouse care. We thank H.-R. Rodewald for providing *Il7ra*^{Cre}Rosa26^{YFP} mice and S.E.W. Jacobsen for fruitful discussions. This work was financed by the Institut Pasteur, INSERM, Pasteur-Weizmann Foundation and ANR (grant Twothyme and Epi-Dev) through grants to A.C.; by REVIVE (Investissement d'Avenir; ANR-10-LABX-73) to A.C. and R.E.; by recurrent funding from the Institut Pasteur, the CNRS, Revive (Investissement d'Avenir; ANR-10-LABX-73) and by an ERC investigator award (2016-StG-715320) from the European Research Council to E.G.P.

AUTHOR CONTRIBUTIONS

R.E. designed and performed most experiments, analyzed data and wrote the manuscript; S.M. analyzed chimeric mice and contributed to discussions. F.S.S. and T.P. performed Biomark analysis. O.B.-D performed neonatal thymectomy. E.G.P., L.F. and L.I. performed fate-mapping experiments. A.B. performed adoptive transfer in neonatal mice. R.G., P.V., A.B. and P.P. contributed to the discussions. A.C. directed the research, designed experiments, analyzed data and wrote the manuscript. All authors contributed to the manuscript.

COMPETING FINANCIAL INTERESTS

The authors declare no competing financial interests.

DATA SHARING

For original data, please contact the corresponding author.

Figure Legends

Figure 1. E13 ETPs retain T/LTi lineage potential in vitro and generate LTi cells in a fetal thymic microenvironment

- Experimental strategy for combined T, B and ILC lineage potential analysis of single ETPs. Single ETPs from either E13 or E18 were sorted onto OP9 stromal cells supplemented with IL-7, Flt3L, KitL and IL-2. After 36 hours, clones were subdivided in conditions that sustain differentiation of T cells (OP9-DL4 supplemented with IL-7, Flt3L, KitL and IL-2) or B, myeloid and ILC/LTi (OP9 supplemented with IL-7, Flt3L, KitL, IL-2 and GM-CSF).
- Representative flow cytometry plots outlining the gating strategy used to identify ILC1, ILC2, ILC3 and NK cells of E13 & E18 ETPs single cell-derived multi-ILC lineage clone.
- Pie chart indicating all phenotypic combinations in individual clones detected after *in vitro* differentiation of E13 (81 clones analyzed out of 240 sorted cells CE 34%) or E18 ETPs (86 clones analyzed out of 240 sorted cells CE 36%) in two independent experiments. CE, cloning efficiency. Frequency of clones generating only T cells (black); T, NK, ILC1, ILC2 and ILC3 (red) (different in E13 and E18 clones $p < 0.0001$); T and LTi (RoRc⁺ CCR6⁺) (blue) (different in E13 and E18 clones $p < 0.0001$); T, NK, LCX two other ILC subsets (orange); T and ILC2 (grey); T and two other ILC subsets (green); T, B and myeloid cells (olive) (different in E13 and E18 clones $p = 0.0036$). All other combinations were not significantly different in E13 and E18 clones.
- Flow cytometry plots of Rag2^{-/-}γc^{-/-} E14.5 thymic lobes reconstituted with 500 E13 ETPs or 500 E18 ETPs per lobe and gated CD3⁻ and stained for the expression of CD127 and CCR6 (left plots). Numbers of double positive (DP) thymocytes per lobe (right plot), Thymic LTi per lobe (middle plot) Vγ5Vδ1 γδT cells (left plot). FTOCs were analyzed at day 12 after reconstitution. **** $P < 0.0001$.
- Single E13 ETP were processed as in (a). After 36-48 hours in culture clones were harvested and colonized single Rag2^{-/-}γc^{-/-} E14.5 thymic lobes. After 24-48 hours in hanging drop lobes were transferred into filters and analyzed at day 12 (n=10 lobes).

Figure 2. E13 ETPs have a transcriptional LTi signature and are required for the maturation (CD80⁺) of mTEC

- Single-cell multiplex qPCR analyzed by hierarchical clustering of single E13 and E18 ETPs (80 cells each) for the expression of ILC lineage specific transcripts (right margin).

Each column represents a cell (E13 ETP in salmon, E18 ETP in blue) and each row represents one gene (of 41 genes). Highlighted are ILCs associated transcripts (black) and LTi associated transcripts (in red). Analysis was done by normalizing expression to two independent house-keeping genes (*Gapdh* and *Actinb*) in R package Phenograph as in (Perchet et al., 2018) and represented in a code color where red represents high expression and blue low expression. Data are pooled from two independent experiments.

- (b) Pregnant females were injected at E10.5, E12.5 and E14.5 with 1 mg of anti-IL-7Ra antibody A7R34 (Red arrows indicate time points of anti-IL-7Ra injections and violet arrows indicate time points of analysis). Thymic lobes were analyzed at E16.5 for the presence of ETP ($\text{Lin}^- \text{CD117}^+ \text{CD44}^+ \text{CD24}^{\text{low}}$), for $\text{V}\gamma 5\text{V}\delta 1 \gamma\delta\text{T}$ cells and for LTi ($\text{CD127}^+ \text{CCR6}^+ \text{TcR}^- \text{CD3}^-$ cells) ($n = 6$) or at P2 for the presence of DN ($\text{CD4}^- \text{CD8}^- \gamma\delta^-$), DP ($\text{CD4}^+ \text{CD8}^+$), CD4^+ thymocytes and of $\text{V}\gamma 5\text{V}\delta 1 \gamma\delta\text{T}$ cells, for LTi ($\text{CD127}^+ \text{CCR6}^+ \text{TcR}^- \text{CD3}^-$ cells) and for CD80^+ mTEC ($\text{EpCAM}^+ \text{Ly51}^- \text{UEA.1}^+ \text{CD45}^-$) ($n = 24$). Plots show numbers of the respective populations per thymus. Data from two independent experiments. **** $P < 0.0001$.

Figure 3. Neonatal thymectomy has no effect on embryonic derived $\text{V}\gamma 5$ and $\text{V}\gamma 6 \gamma\delta$ T cells

- (a) Schematic diagram of neonatal thymectomy experiment. P1 newborn mice were thymectomized and analyzed 6 weeks later.
- (b) Frequencies of double positive CD4/CD8 T cells found in the thymus and peri thymic tissue isolated from sham and thymectomized mice, respectively.
- (c) Number of $\text{V}\gamma 5^+ \gamma\delta$ T cells in the epidermis isolated from one ear of sham and thymectomized mice.
- (d) Number of $\text{V}\gamma 6 \text{IL17} \gamma\delta$ T cells, $\text{V}\gamma 4 \text{IL17} \gamma\delta$ T cells and $\alpha\beta$ T cells in one inguinal lymph node, isolated from sham and thymectomized mice.
- (e) Number of $\alpha\beta \text{CD4}^+ \text{CD44}^-$ T cells in the spleen. * $P < 0.05$, ** $P < 0.01$ and *** $P < 0.001$ (Student's *t*-test). Data are representative of at least 4 mice in each group from two independent experiments. Data are depicted as mean \pm s.e.m.

Figure 4. Emergence of $\text{IL7R}\alpha^+$ expressing YS-progenitors in E9.5 embryos

- (a) Schematic representation of the anatomical sites analyzed in mouse embryos: YS, head, fetal liver and the AGM region.
- (b) Representative flow cytometry plot showing YFP expression on live $\text{Lin}^- \text{CD117}^+ \text{CD41}^+$ E9.5 YS cells from $\text{Il7r}^{\text{cre}} \text{ROSA26}^{\text{LSLYFP}}$.
- (c) Number and Percentage of YFP⁺ per YS (mean \pm s.e.m). Data representative of 14 embryos from 4 independent experiments.
- (d) Representative flow cytometry plot showing YFP expression on live $\text{Lin}^- \text{CD117}^+$ E9.5 placenta and AGM region cells.
- (e) Expression of CD115, CD127, CD135, CD16/32 and CD31 within the E9.5 YS $\text{Lin}^- \text{CD117}^+ \text{CD41}^+ \text{YFP}^+$ and YFP^- populations.
- (f) Experimental strategy for single cell lineage potential assay of E9.5 YS $\text{Lin}^- \text{CD117}^+ \text{CD41}^+ \text{YFP}^+$ and YFP^- populations.
- (g) Frequency of wells containing B cells or (h) T cells in cultures of single sorted E9.5 YS $\text{Lin}^- \text{CD117}^+ \text{CD41}^+ \text{YFP}^+$ and YFP^- cells (180 cells from each population analyzed in three independent experiments).
- (i) Frequency of erythroid and megakaryocytic (E/Mk), myeloid (GM) or mixed E/Mk/GM colonies of single sorted E9.5 YS $\text{Lin}^- \text{CD117}^+ \text{CD41}^+ \text{YFP}^+$ and YFP^- cells.

- (j) Frequency of thymic lobes irradiated and reconstituted with CD117⁺ E9.5 YS YFP⁺ or YFP⁻, or with E12.5 LSK or E10.5 YS as controls, that contained CD4/CD8 DP cells (left plot) or TCR-V γ 5⁺ T cells (right plot). FTOCs were analyzed at day 12 after reconstitution.

Figure 5. Gene expression analysis of single E9.5 YS Lin⁻ CD117⁺ CD41⁺ YFP⁺ and YFP⁻ cells.

- (a) Single-cell multiplex qPCR analyzed by hierarchical clustering of single YFP⁺ (47 cells) and YFP⁻ (10 cells) E9.5 Lin⁻ CD117⁺ CD41⁺ cells analyzed for the expression of lymphoid associated (*Il7r*, *Rag1*, *Rag2*, *Flt3*), myeloid associated (*Cebpa*, *Cd32*, *Csf1r*, *Csf2r*, *Csf3r*, *Irf8*, *Pu1*), B cell associated (*Pax5*, *Ebf1*), E/Mk associated (*EpoR*, *Gata1*, *Mpl*, *Tal1*, *Vwf*, *Klf1*) and hematopoiesis associated (*Gata2*, *Myb*, *Runx1*, *Kit*, *Cd34*) genes.
- (b) Number of *Il7r*⁺ and *Il7r*⁻ cells within E9.5 YS YFP expressing cells.

Figure 6. Thymopoiesis-initiating cells develop exclusively from HSC-derived progenitors

- (a) Experimental design of lineage tracing analysis of *Csf1r*-expressing cells after OH tamoxifen (OH-TAM) administration at E8.5, or E9.5, or E10.5. Arrows indicate pulse and analysis time points.
- (b) Flow cytometry analysis of E12.5 early thymic progenitors (ETPs). E12.5 thymic lobes of embryos pulsed at indicated time points were analyzed. Left plots show the gating strategy to identify ETP. Right representative histograms showing the frequency of Tomato⁺ or YFP⁺ cells in ETP. For each experiment one representative analysis is shown.
- (c) Frequencies of YFP or Tomato labelled hematopoietic progenitors and Lymphoid tissue inducer (LTi) in E12.5 fetal liver, FB and thymi (left plots) and of LSK, B1 B cells, B cells and V γ 5⁺ T cells in adult tissues (right plots) of animals pulsed at E8.5, E9.5 or E10.5. Microglia served as controls for labelling efficiency.

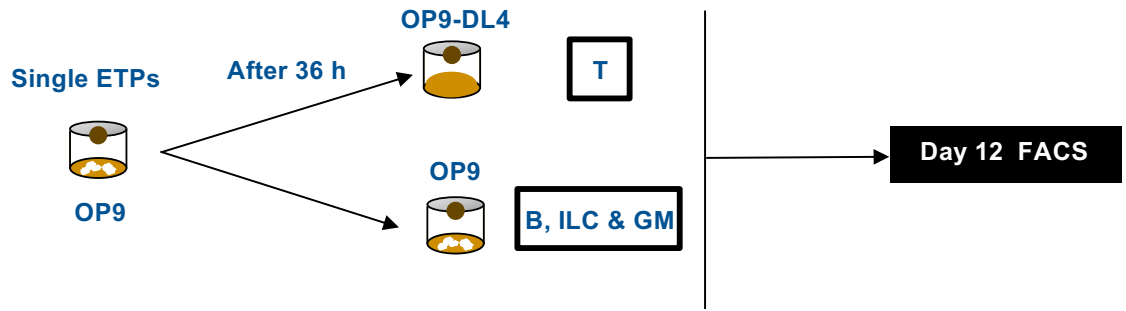
All data are pooled from minimally two independent experiments, for embryos analyzed at E12.5 (pulsed at E8.5, n = 8; E9.5, n = 10; E10.5, n = 10) and for adult tissues animals were analyzed between 10-12 weeks of age (pulsed at E8.5, n = 6; E9.5, n = 6; E10.5, n = 2). Data are depicted as mean \pm s.e.m except for adult animals pulsed at E10.5 (mean). Abbreviations: ETPs, early thymic progenitors; PerC, peritoneal cavity; BM, bone marrow; FB, fetal blood; FL, fetal liver; FT, fetal thymus.

Figure 7. Model depicting the origin and the lineage potential of thymopoiesis-initiating progenitors.

Abbreviations: ETPs, early thymic progenitors.

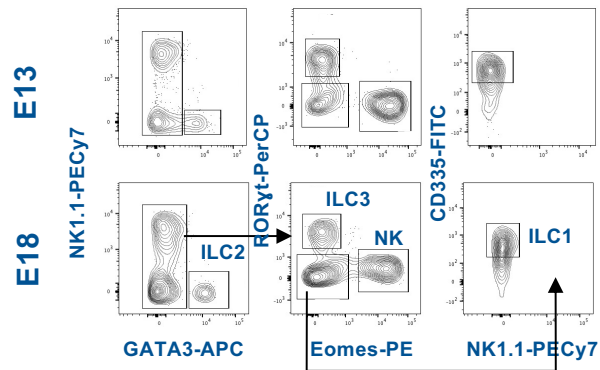
Figure 1

a

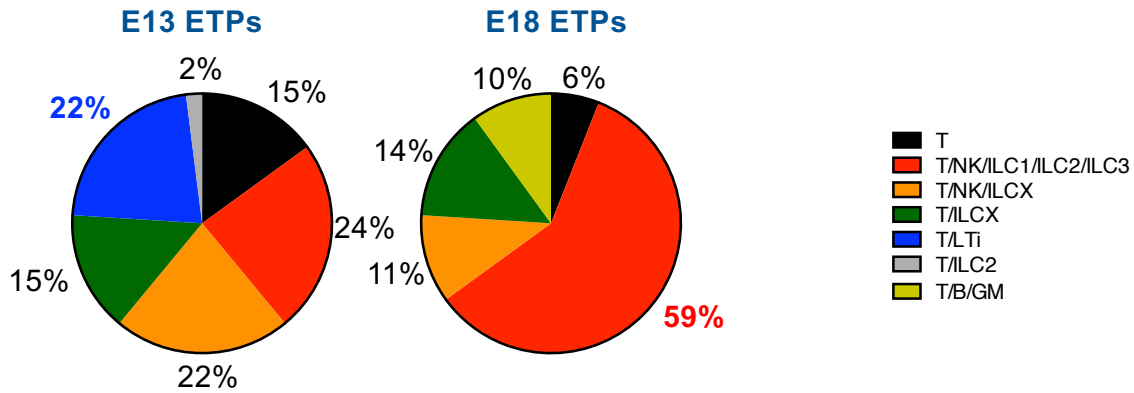


b

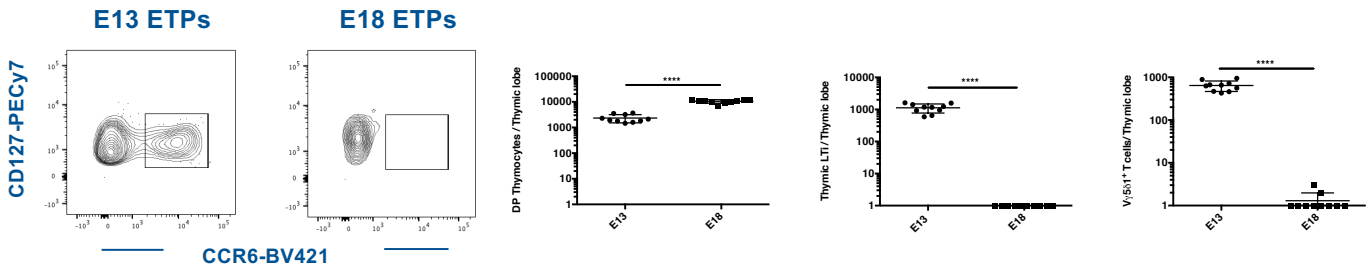
In vitro Multi-ILC lineage potential from single ETPs



c



d



e

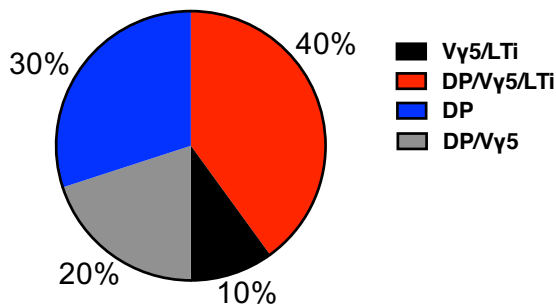


Figure 2

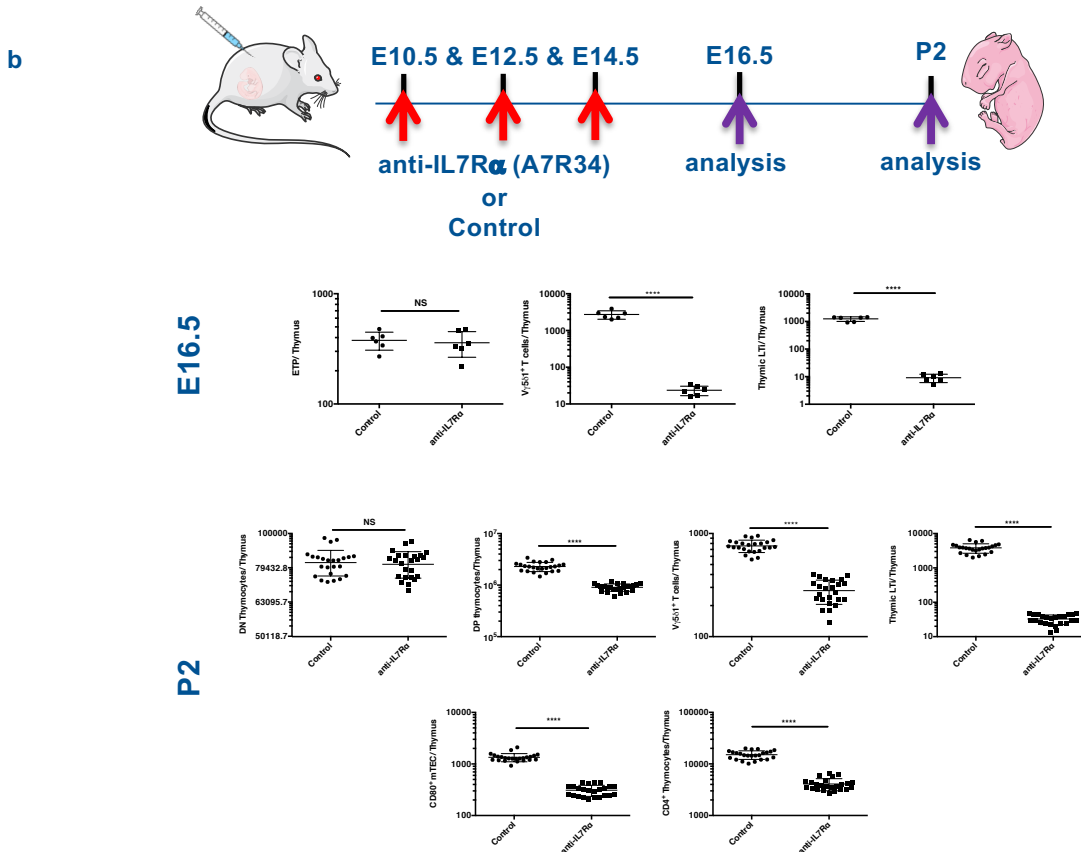
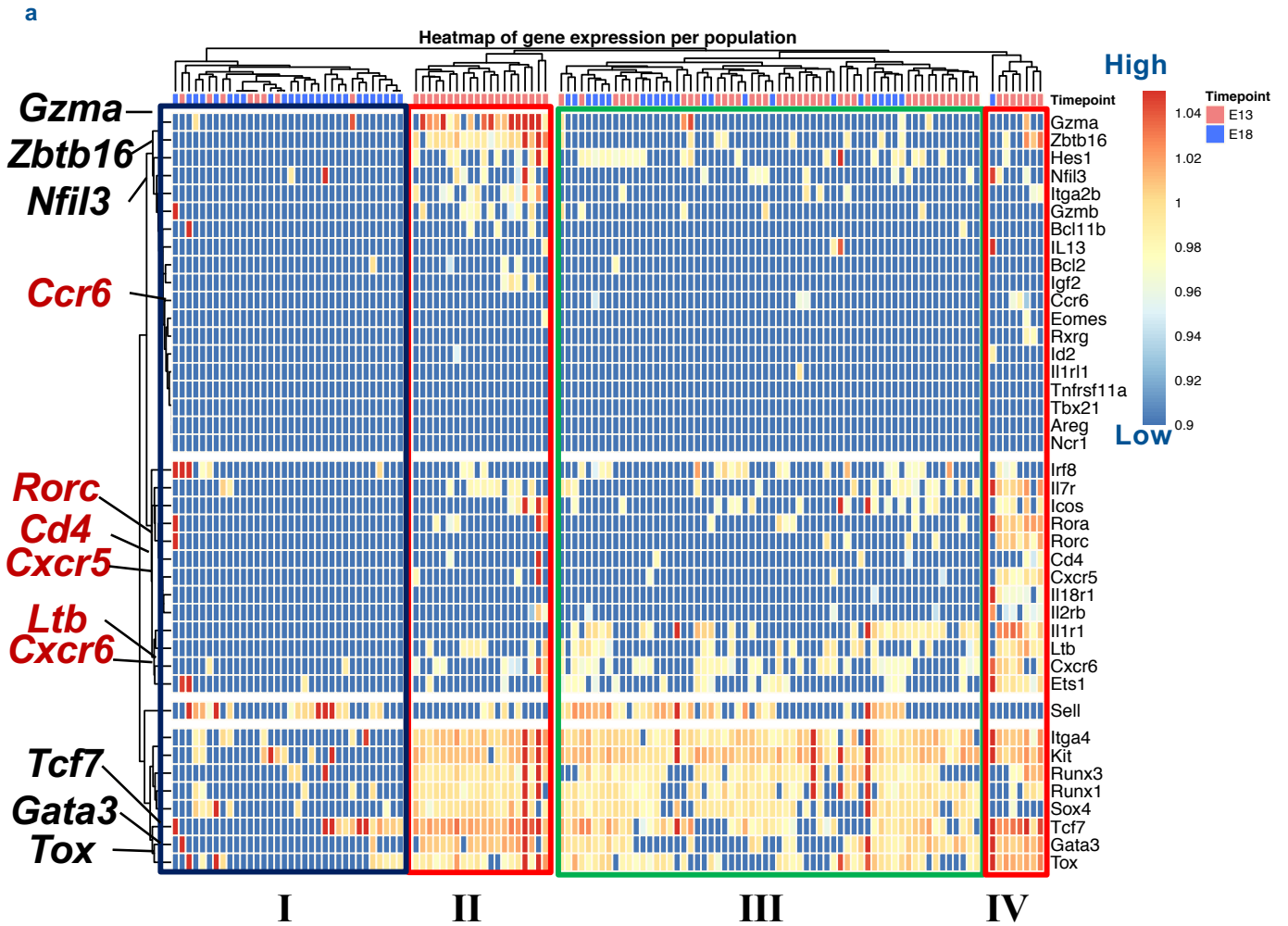


Figure 3

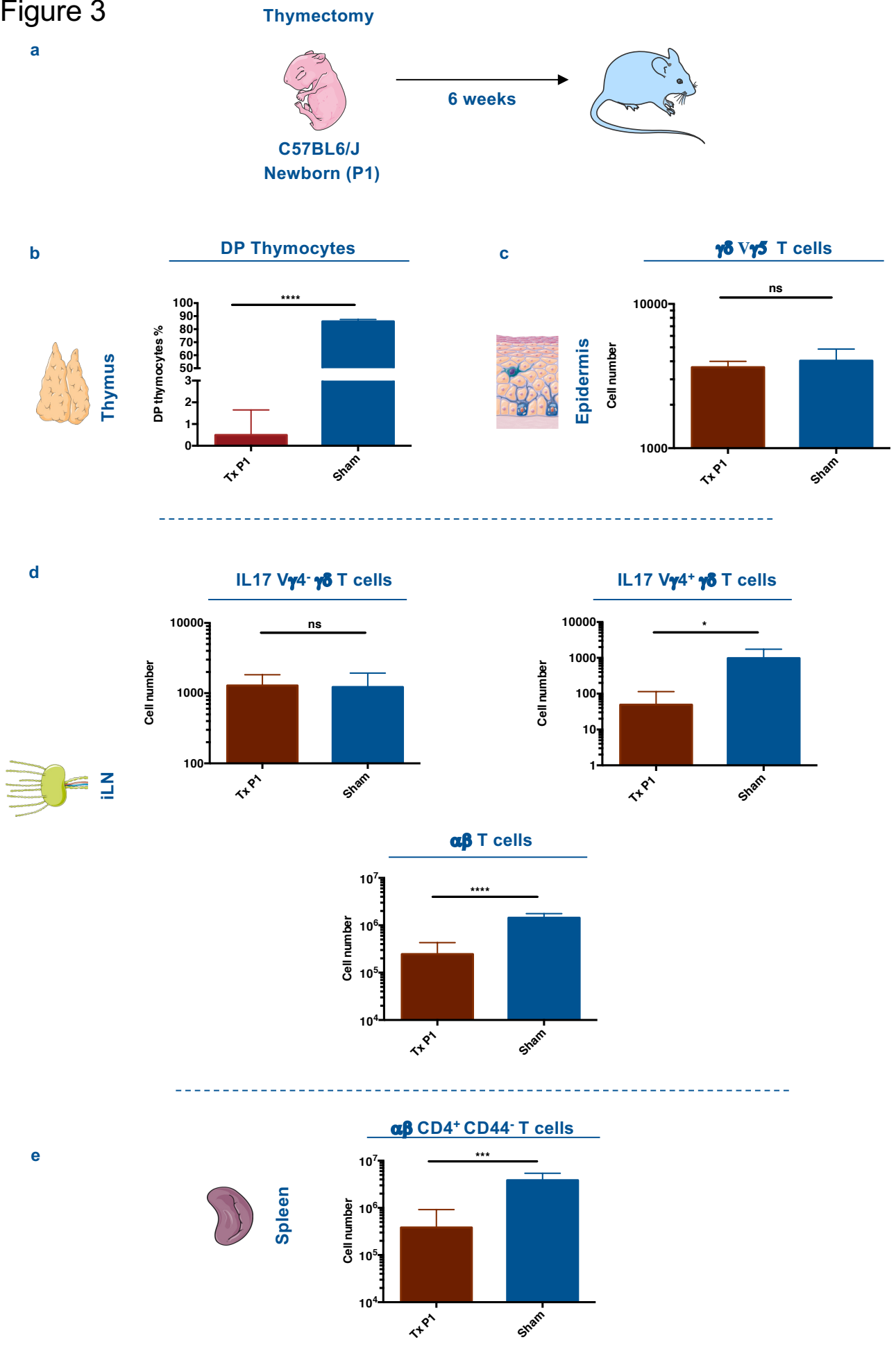
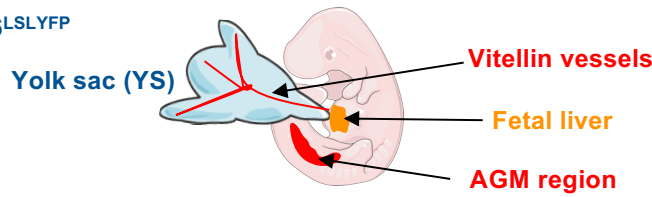
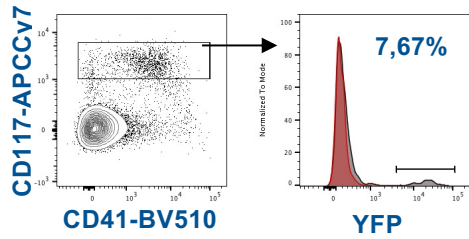


Figure 4

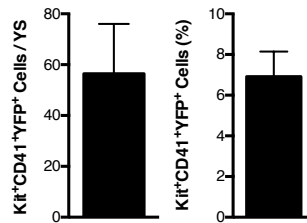
a *I17^{cre}ROSA26^{LSL}YFP*



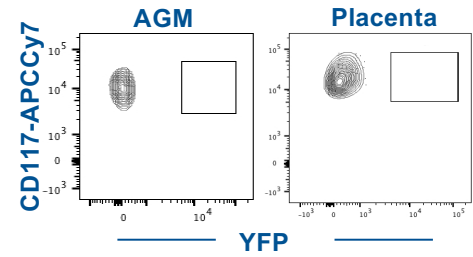
b **Lin⁻ YS E9.5**



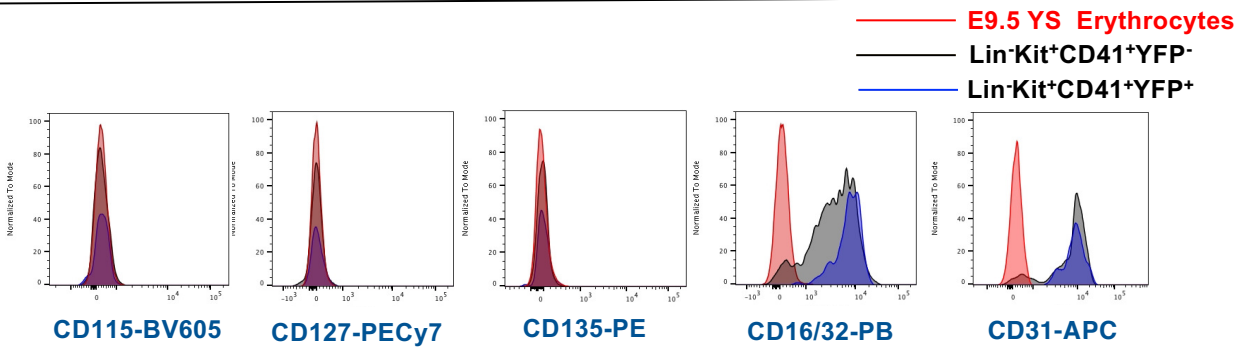
c



d **Lin⁻ Kit⁺ E9.5**



e **E9.5 Lin⁻ Kit⁺ CD41⁺**



f **Day 1 Single cell**

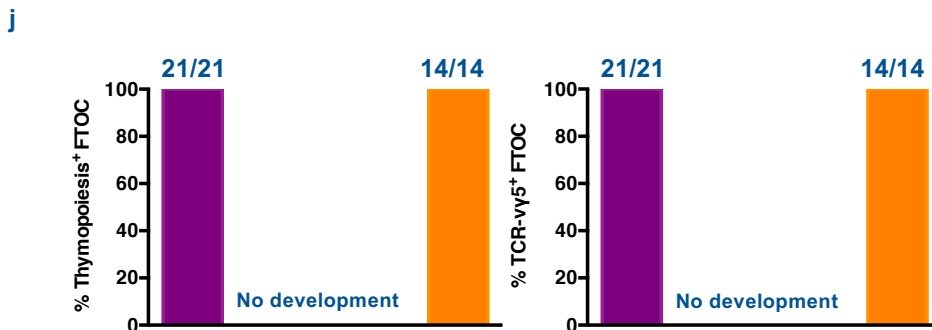
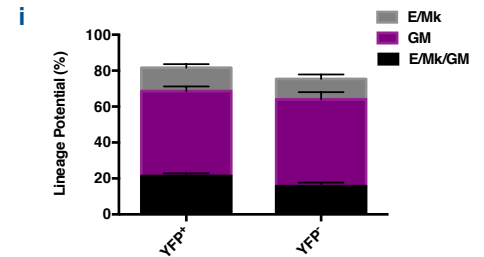
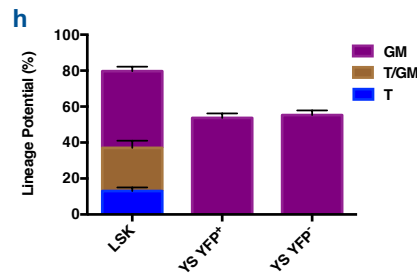
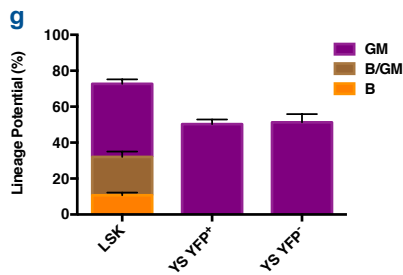
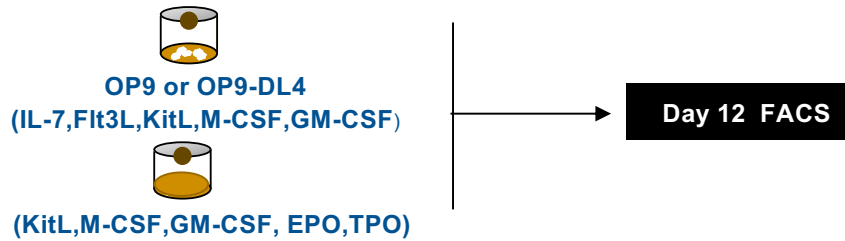
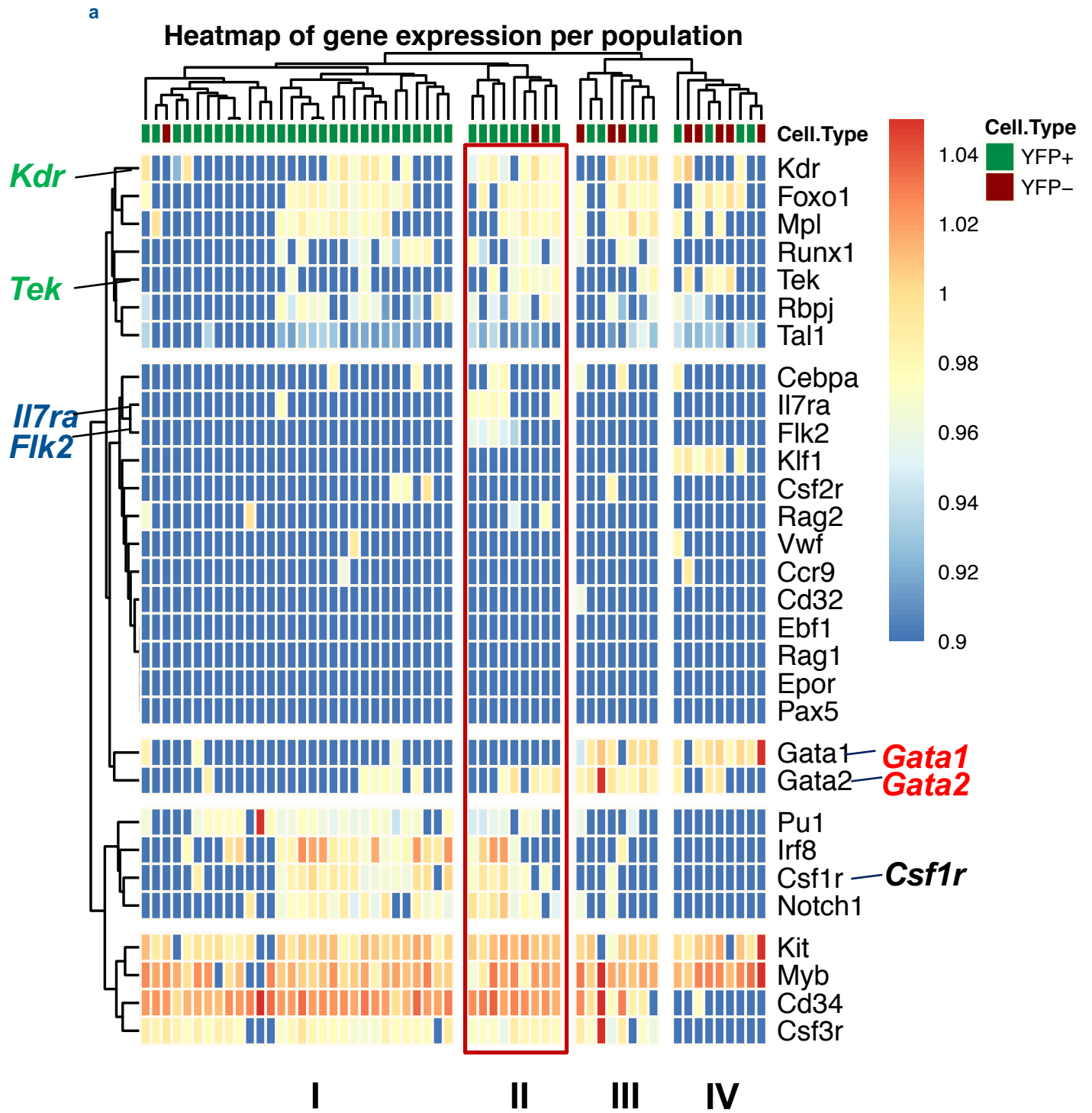


Figure 5



b

	YFP +
<i>Il7r</i> ⁺	6
<i>Il7r</i> ⁻	41

Figure 6_a

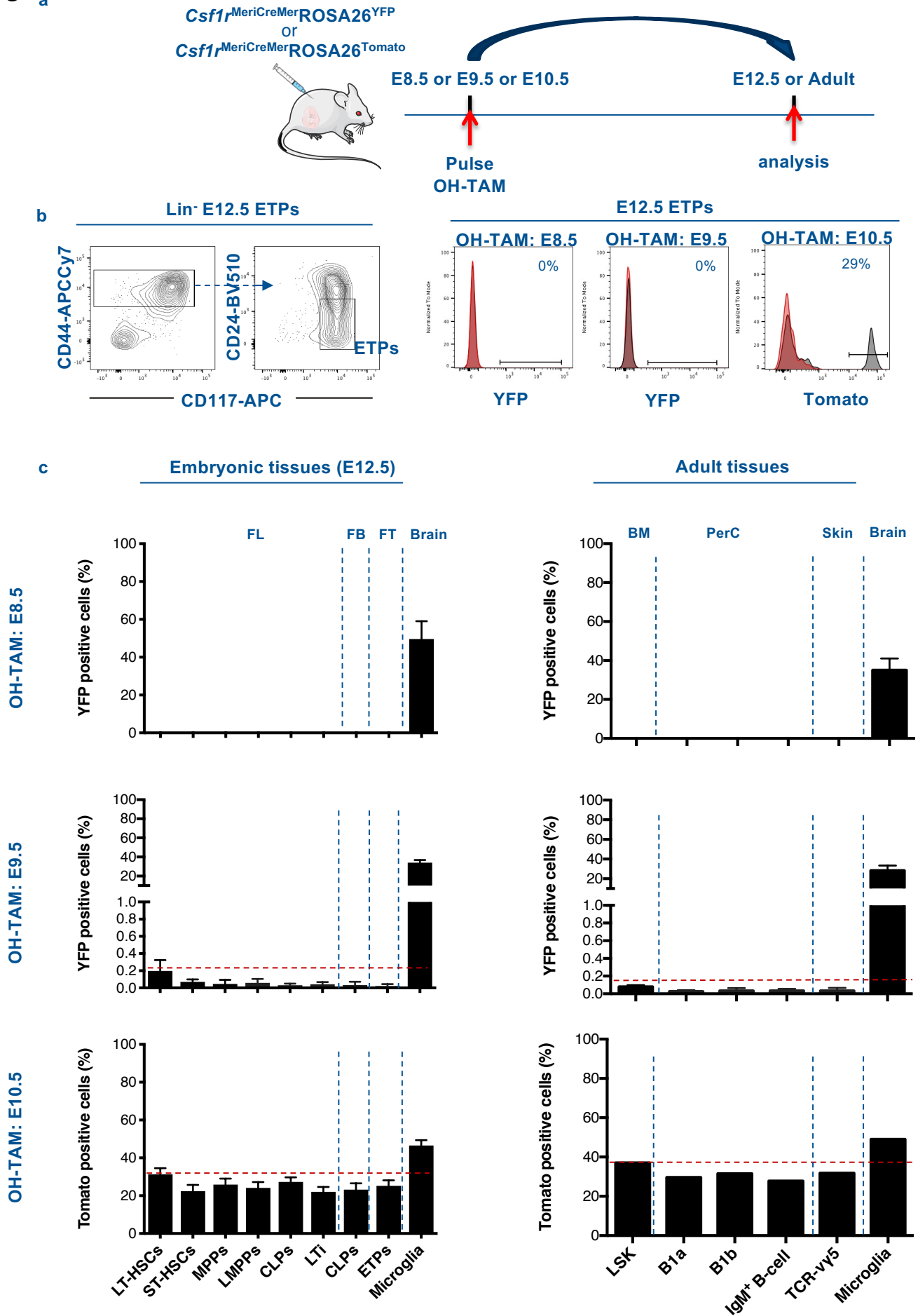


Figure 7

